



OPEN

Psychometric evaluation of high-resolution electrotactile interface for conveying 3D spatial information

Tanja Boljanić^{1,2✉}, Milica Baljić¹, Miloš Kostić¹, Pierre Barralon³, Strahinja Došen⁴ & Matija Štrbac¹

This study presents a detailed psychometric evaluation of a novel high-resolution electrotactile interface, which is developed to provide users with 3D spatial information and facilitate enhanced interaction with a Supernumerary Robotic Limb (SRL). The research introduces a novel electrotactile system that employs a multi-pad electrode configuration on the thigh, aimed at delivering intuitive feedback to users about the position of the SRL in a three-dimensional space. The interface's effectiveness was assessed through a series of psychometric tests, including static spatial discrimination, target-reaching with spatial feedback, frequency discrimination, and combined spatial/frequency modulation. The key findings demonstrate that participants could differentiate between 30 electrode pads with an average success rate of 62.7% when they were activated statically, while in the dynamic target-reaching task, the success rate increased to 88.1%. Frequency discrimination tests further revealed that four frequency levels could be distinguished with 86.0% success rate in single-pad feedback while the performance decreased to 74.3% in multi-pad distributed feedback. Finally, in the closed-loop test with mixed spatial and frequency modulation, participants achieved an overall success rate of 78.8% in target reaching across 10 × 4 discrete 2D space. These results highlight the interface's capability to transmit high-resolution spatial information through electrotactile feedback, offering a foundation for future applications in tactile-based navigation and control systems.

Electrotactile stimulation is a well-known technique for conveying sensory information through electrical signals delivered directly to the skin¹ to depolarize skin afferents and thereby elicit tactile sensations². The produced sensations can vary from a light tingle, over tickling to more pronounced pricking sensations, depending on the intensity and frequency of the electrical current³. Due to their affordability, low power consumption, lightweight design, silent operation and short response time, electrotactile systems provide several advantages over other forms of haptic feedback relying on mechanical elements that need to be accelerated and moved⁴.

Electrotactile stimulation can be used to provide real-time feedback in different applications, from medical rehabilitation to advanced human-machine interaction. It holds promise for improving grasp control in hand rehabilitation⁵, and restoring the sense of touch in stroke patients or amputees⁶. In the latter application, for instance, it is used to convey proprioceptive and force feedback from a myoelectric prosthesis^{7–11}. Electrotactile stimulation is also utilized to provide tactile feedback in tele-robotics^{12–14} and virtual reality^{15,16}. Similarly, this approach is of particular interest within the NIMA project¹⁷, where the goal is to provide real-time feedback to the user about the state of the Supernumerary Robotic Limb (SRL), a wearable robotic device attached to the human body to extend human capabilities¹⁸. Sensory feedback can have significant impact on SRL control (e.g., improvement in force regulation, accuracy and task completion time) and embodiment (e.g., mitigation of feedback discrepancies and human-robot kinematics)¹⁹. Previous studies relied on electrotactile stimulation delivered to the contralateral thumb to convey information on contact force from a supernumerary robotic digit^{20,21}. However, lower limb might be a better target for delivering feedback, as it minimizes interference

¹Tecnalia Serbia doo, 11000 Belgrade, Serbia. ²School of Electrical Engineering, University of Belgrade, 11000 Belgrade, Serbia. ³TECNALIA Basque Research and Technology Alliance (BRTA), 20009 Donostia-San Sebastián, Spain. ⁴Department of Health Science and Technology, Aalborg University, 9260 Gistrup, Denmark. ✉email: tanja.boljanic@tecnalia.com

with natural proprioception from the upper limbs that can be also employed in the task at hand or even used for controlling the SRL^{22,23}.

Modern electrotactile systems often employ multi-channel interfaces, enabling a more diverse and enriched set of tactile sensations. In this case, the information can be conveyed by combining spatial and parameter modulation and thereby changing the stimulation site and the number of active channels, as well as the duration, width, frequency, and amplitude of the electrical pulses^{7,24}.

Research into the spatial resolution of electrotactile stimulation applied to the thigh is limited and shows conflicting results. The reported two-point discrimination threshold (TPDT) for thigh stimulation varies significantly, from 9.88²⁵ to 57.85 mm²⁶. Furthermore, the psychometric evaluation in the previous studies was limited to a maximum of eight channels^{26,27}. The spatial discrimination using an eight-channel electrotactile stimulator yielded different average recognition rates: from 64.55% reported by Vallete et al.²⁶ to the substantially higher 98% according to Webb et al.²⁷.

This paper presents a series of psychometric experiments that were performed successively to evaluate a novel high-resolution electrotactile interface for the thigh of prospective users (artificial proprioceptive feedback)²², as conceptually shown in Fig. 1. Feedback was designed to convey information about the position of the SRL in a three-dimensional (3D) space by coding two dimensions in stimuli location and the third in stimulation frequency. The tests assessed user understanding of the coding, the presented dimensions, and their combinations in real-time control, with the focus on two closed-loop 2D target reaching tasks that showcase feasibility in future application in the 3D space. In the first step, we assessed the static spatial discrimination (SD) of active pads distributed in three rows circularly around the thigh. In the following stage we examined the closed-loop control scenario during “tactile” target teaching task (TR), where the feedback was provided using spatial modulation (Target Reaching Spatial—TR-S). The next step was to investigate differences in frequency discrimination (FD) during a single pad (FD-SP) and a multi pad (FD-MP) use of the electrode. The final assessment presented in the manuscript integrates the two approaches and evaluates the use of mixed spatial and frequency modulation (MSF) to provide intuitive position feedback in a polar coordinate system in the “tactile” target-reaching task (TR-MSF). The experiments were conducted successively, aiming to address the following hypotheses:

H1 Dynamic encoding during closed-loop control (TR-S) will provide a superior understanding of stimuli position compared to static recognition (SD).

H2 Static recognition of frequency across multiple pads (FD-MP) poses a greater challenge compared to the single pad stimulation (FD-SP).

H3 The additional modulation of frequency in combined dynamic encoding during closed-loop control (TR-MSF) will not affect the accuracy of spatial discrimination obtained in static conditions (TR-S).

Methods

Setup

The experimental setup included (Fig. 2a):



Fig. 1. The envisioned application of controlling the SRL end effector position in 3D space by relying on the high-resolution electrotactile interface providing the tactile feedback on the thigh of the subject.

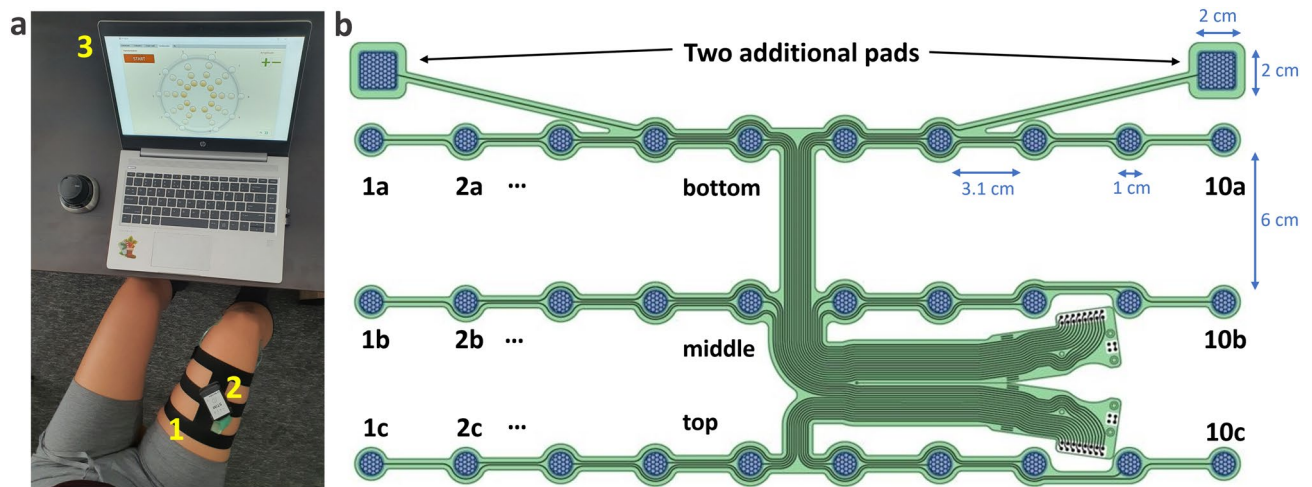


Fig. 2. The experimental setup. (a) The setup comprised a custom-designed multi-pad electrode (1), a stimulator unit (2), and a laptop (3). (b) Technical design of the multi-pad electrode with annotated pads and rows.

- (1) A custom-designed multi-pad electrode for the thigh,
- (2) A multi-channel programmable stimulator with a Bluetooth communication interface,
- (3) A laptop with a custom application developed in MATLAB R2019b (The MathWorks, Inc., United States).

The multi-pad electrode (Fig. 2b) was designed and developed to provide tactile feedback from an SRL to the thigh of the subject based on previously reported values of two-point discrimination threshold and the results of pilot tests on return electrode configuration and active electrode discrimination²². It features three arrays (6 cm edge-to-edge distance) each consisting of ten circular pads (1 cm in diameter, 3.1 cm edge-to-edge distance) and two square pads (2 cm × 2 cm each). The three arrays were designed to provide spatial feedback, as described later, while the two extra pads were envisioned as an independent information channel for transmitting discrete messages, such as alerts and warnings in critical situations. The electrode prototypes were produced by screen printing of conductive and dielectric inks for biomedical applications on a flexible transfer film (Policrom, IT²⁸) and the pads were coated with PEDOT:PSS. The electrode was heat transferred to a custom prepared (i.e., by laser cutting) neoprene band with the Velcro fabric for easy attachment.

The 32-channel stimulator unit (previously developed by Tecnia Research & Innovations, ES within the TACTILITY project²⁹) was used to generate current-controlled rectangular symmetric biphasic pulses with amplitude in the range of 0.1–9 mA (0.1 mA step). The stimulator unit was linked to the laptop via a Bluetooth interface, enabling real-time control over stimulation parameters (0.1–9 mA amplitude with 0.1 mA step, 30–4000 μ s pulse width with 1 μ s step and 1–500 Hz pulse rate with 1 Hz step) as well as the selection of the electrode pads to be set as “active” and “return” electrodes in each stimulation pulse. In biphasic stimulation, “active electrode” denotes a pad intended to produce tactile sensation, while the “return electrode” denotes a group of pads of significantly larger combined contact surface which close the electrical circuit without eliciting sensations below them (due to significantly lower current density). In this study, the return electrode configuration was selected based on the results of pilot tests²². Specifically, if the pad from the bottom or top array was active, the return electrode consisted of all pads from the middle array, whereas in case of an active pad from the middle array, all pads from the bottom array served as the return electrode. The stimulation frequency and the pulse width were set to 30 Hz and 300 μ s, respectively. These parameter values were adopted from prior studies^{22,30} to ensure that the induced sensations were comfortable and could be finely modulated in intensity by changing the pulse amplitude using 0.1 mA increment, which was corroborated by our pilot tests.

Subjects

A total of 32 subjects participated in our experiments. For the SD test, we recruited 10 subjects (gender: 5/5 females/males; age: 27.5 ± 4.6 years). Another group of 10 subjects, matched in gender and age, participated in the TR-S test (gender: 5/5 females/males; age: 27.0 ± 4.1 years). For the FD test, we recruited an additional 12 participants (gender: 5/7 females/males; age: 27.8 ± 4.8 years). Among these, 10 subjects also participated in the TR-MSF test (gender: 4/6 females/males; age: 28.2 ± 5.8 years).

All participants were screened to ensure they had no musculoskeletal or somatosensory disorders and no visible skin damage on their thighs. Before participating in the experiments, the subjects were provided with an information sheet explaining the methods and objectives of the study and they signed an informed consent form. The study was conducted following the Declaration of Helsinki and the experimental protocol was approved by the ethics committee of the University of Belgrade—Faculty of Medicine, Serbia (protocol code 1322/III-19, date of approval 17 March 2021).

Protocol

For all tests, the subjects were seated comfortably at a table, facing a laptop running one of the custom MATLAB applications developed for each of the four tests (Fig. 2a). The electrode was centred on the mid-anterior region of the right thigh, with three arrays distributed around the thigh. The bottom array was positioned 10 cm above the upper edge of the knee. Two additional square pads were positioned 7 cm distally from the bottom array, on the medial and lateral sides of the thigh. Prior to the electrode placement, the subject's leg was moistened with water and then dried with a paper towel. The stimulator unit was attached on the mid-anterior thigh, just above the middle array.

The experimental protocol for all tests included four phases: calibration, familiarization, reinforced learning, and validation. At the end of each phase, the participants were instructed that they could choose to proceed to the next phase when they felt ready. The calibration phase aimed to fine-tune the current amplitude for each pad, ensuring the tactile sensation was distinct, comfortable, and localized beneath the active pad. For the selected set of pads used in the test, the subject was asked to increase the stimulation amplitude by 0.1 mA until they perceived the sensation below the active pad (i.e., sensation threshold—ST). The localization threshold (LT) was then estimated from the ST, as explained in²², and the procedure was repeated for each pad. In the end, the subject was asked to activate all pads sequentially and confirm that the sensation was clear and localized below the pad or readjust the amplitudes where necessary. In the FD and TR-MSF tests, where frequency modulation was used, the subjects tested the perceived sensations across all frequency levels and adjusted the amplitude if required. Amplitude values established in the calibration phase were used throughout all subsequent phases. The subjects did not report the loss of sensitivity due to habituation during the experiment, which is likely due to the dynamic nature of the protocol (habituation is most expressed during prolonged constant sensations). The remaining phases were specific for each test and are therefore explained in detail in the following subsections. The familiarization phase served to acquaint subjects with electrotactile sensations and the nature of tactile feedback. The task in reinforced learning was to train the subjects to interpret the feedback. This was done by asking the subject to perform the task and then providing feedback on the correct result. The subjects advanced to the validation phase regardless of their results in the reinforced learning. The validation phase was the actual assessment of performance. The task in this phase was the same as in the reinforced learning but without the subsequent feedback on the goal achievement. The structure and timeline of the experiments presented in the study are illustrated in Fig. 3. In the closed-loop tests, we utilized two control interfaces: a keyboard for TR-S and a SpaceMouse for TR-MSF, as detailed further in their respective subsections.

Spatial discrimination test

We designed the SD test to assess subjects' ability to distinguish among the 30 pads distributed on the thigh. In the familiarization phase, the pads were activated sequentially from pad 1a to pad 10c (following the labelling in Fig. 2b) while visual feedback was provided on the screen (the activated pad was coloured green on the electrode drawing). Each pad was activated for 2 s with 1.5 s pause between the activations. The sequence of 30 pads was repeated three times.

In the reinforced learning phase, the subjects were asked to identify a randomly activated pad by selecting the pad on the electrode drawing displayed on the screen. If the subject answered correctly, the pad was coloured green, otherwise, the correct pad was indicated in red. Each pad was activated for 3 s and visual feedback was provided for 1 s following the subject's response. The sequence of 30 pads was activated five times, each time using a new pseudo-random order.

The validation phase followed the same protocol as in the reinforced learning, but the subject did not receive visual feedback on their responses. In total, the experimental session lasted between 60 and 90 min.

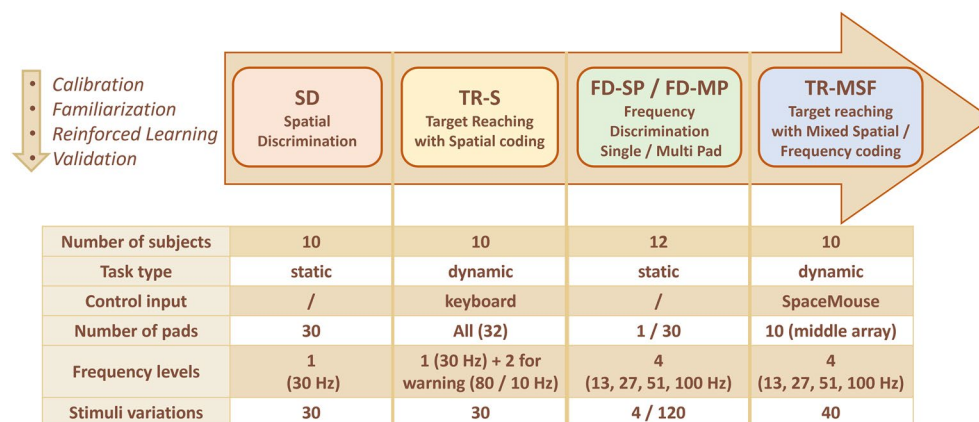


Fig. 3. Timeline and details of four conducted tests (task type, control mechanism, number of subjects, pads, frequencies, and stimuli). Each test comprised calibration, familiarization, reinforced learning, and validation phases.

Target-reaching test with spatial feedback

The TR-S test was conducted to evaluate the subject's ability to navigate across the electrode rows and columns, representing a 2D position of an SRL in the envisioned application, while relying on the electro-tactile feedback. Subjects used a keyboard to navigate through the electrode rows and columns to reach the target by pressing the up-down and left-right arrows, respectively. A 3×10 grid which corresponded to the electrode design was shown on the monitor (Fig. 4) and the subjects were asked to navigate a virtual cursor to the target position, while the current cursor position (grid cell) was conveyed using electro-tactile stimulation. One press to an arrow moved the cursor to the next cell in the direction of the arrow.

In the familiarization phase, the cursor automatically moved through the grid between randomly selected starting and target locations, while its current position (grid cell) was presented visually and conveyed by the electro-tactile feedback (Fig. 4). The active pads were always selected following the shortest path, prioritizing reaching the target row before adjusting its column position. Each pad within the sequence was activated for 1 s. In total, the subjects were presented with 30 randomly generated sequences, with 1 s pause between them.

In the reinforced learning, the subjects were asked to reach the target pad marked on the screen, starting from the random pad that was activated to indicate the starting position. Importantly, in this condition, the visual feedback of the cursor position was not shown to the subject. The stimulation of each pad lasted for as long as the cursor remained within the same grid cell. The feedback also incorporated the alerts indicating that the cursor moved outside the grid boundary. Specifically, upon moving distally from the bottom array and proximally from the top array, the two additional squared pads (Fig. 4a) were simultaneously activated with the amplitude of 2 mA, pulse width of 300 μ s and the frequency of 80 and 10 Hz, respectively. When the subjects judged that the target pad was reached, they indicated this by pressing the enter key. If the subject reached the correct target pad, it was colored green, otherwise, the correct pad was indicated in red. Following the 1.5 s pause, the next trial started by activating a random starting pad and indicating the pseudo randomly selected target pad on the screen. The test included 90 trials, with each of the 30 pads within the grid set as the target for three times.

In the validation phase each of the 30 pads was set as the start and the target for five times, resulting in 150 trials. The experimental session lasted between 60 and 120 min.

Frequency discrimination test

This test was conducted to explore the subject's ability to discriminate between four frequency levels (13, 27, 51, 100 Hz). The FD test included a single pad (FD-SP) and a multi pad (FD-MP) sessions. In the FD-SP session, the same electrode pad was repeatedly activated, whereas in the FD-MP session, each of the 30 pads was activated in a random order. It should be noted that the location of the active pad was not of interest in this study and the subjects were asked to focus only on recognizing the frequency level, regardless of the active pad. The subjects were divided into two groups, one group starting with FD-SP and the other with FD-MP, to exclude the effect of learning. The frequency levels were chosen based on the range of interest and Just Noticeable Difference (JND) curve observed in the forearm experiments⁸ and confirmed for the thigh in pilot tests.

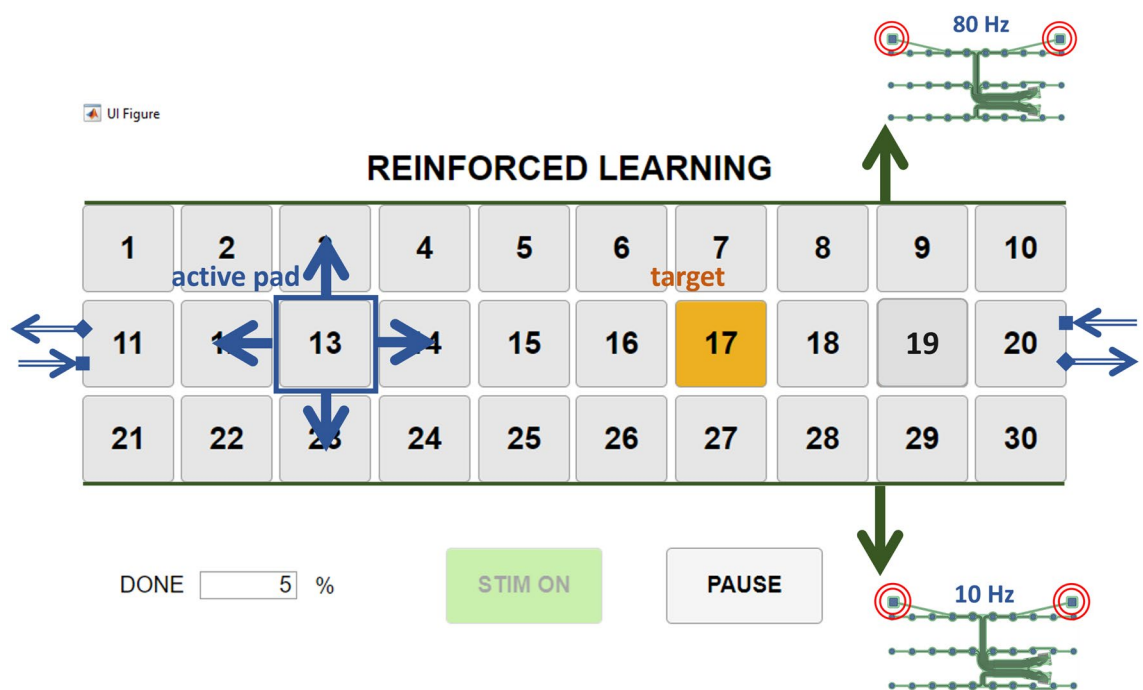


Fig. 4. Visual representation during closed loop tests in the TR-S task: Left/right and forward/backward keyboard arrows were used for control. Warnings pads were activated if the subject moved the cursor out of the grid.

During the familiarization phase in FD-SP, the electrode pad (randomly chosen for each subject) was activated sequentially at different frequencies, from the lowest (13 Hz) to the highest (100 Hz). Visual feedback was displayed on the screen via colour bar, where the darker shade corresponded to the higher frequency. Each frequency level was presented for 2 s, followed by a 1 s pause and the sequence was repeated 30 times. The same pad was used in all trials. In FD-MP, the frequency levels were presented in the same way, but the active electrode pads changed in a pseudorandom order (4 levels \times 30 pads) across trials. The active electrode pad and frequency level were indicated on the screen to provide visual feedback to the subject.

In the reinforced learning phase, the subjects were asked to identify the frequency level by pressing the corresponding button (section of the colour bar) on the screen. Correct responses were indicated by coloring the button green, while in case of incorrect responses, the correct answer was marked in red. The stimulation lasted for 2 s, and the subject could answer during or after the stimulus. The visual feedback about the correct answer was displayed for 1 s after the subject's response, followed by the activation of another stimulus. Each frequency level was repeated 15 times, resulting in 60 stimuli (4 levels \times 15 repetitions). Notably, in FD-MP, the subjects were asked to identify only the frequency level, not the activated pad.

The validation phase followed the same protocol (including the same number of trials) as the reinforced learning phase, but no visual feedback was provided. Outcome measures in the FD-MP test were focused on the identification of the correct frequency, rather than the pad location. In total, the experimental session lasted between 17 and 27 min for FD-SP and between 21 and 44 min for FD-MP.

Mixed spatial/frequency test

This test was designed to evaluate how effectively the subjects could utilize electro-tactile feedback that combines spatial and frequency modulation to complete a target-reaching task. For conveying the 3D position information, representing the SRL end-effector in the target scenario, we have designed an intuitive mapping based on the cylindrical coordinate system. The three coordinates, i.e. radial distance ρ , radial angle φ and axial coordinate or height z , are directly encoded by the stimulation frequency, electrode column and electrode row, respectively (Fig. 5). The radial distance ρ is represented by four frequency levels, where the highest frequency level corresponds to the minimal distance from the origin point. This mapping was selected based on pilot tests in which the sensation of frequency increase was by majority of subjects declared to evoke sensations associated with stimuli distant from the skin and closer to the imagined centre of the leg cross section, thus corresponding to the origin point in the coordinate system. The radial angle φ is represented by one of the ten electrodes in the row that are almost completing the circle around the leg. The axial coordinate z is represented by one of the three electrode rows.

To avoid excessive session duration, only a single row of electrodes was used for this test, corresponding to the movement of the SRL across the transversal plane. The visual representation of the plane, with positions in the polar coordinate system encoded by all combinations of pads (radial angle) and frequency (radial distance), was

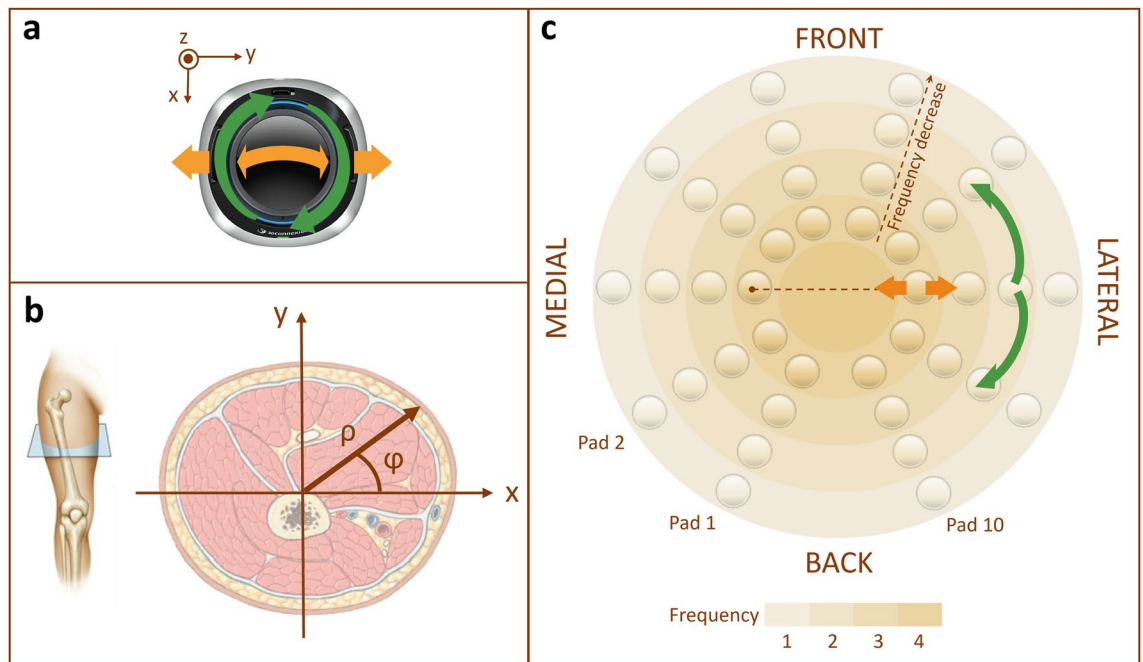


Fig. 5. Visual representation during closed loop tests in TR-MSF task: (a) The SpaceMouse control inputs are presented with green and orange arrows, (b) the cross-sectional view of the thigh overlay with the polar coordinates—radial distance (ρ) and radial angle (φ) that are used for intuitive feedback mapping and (c) graphical feedback of 10 spatial \times 4 frequency levels with green and orange arrows denoting corresponding movements. The cross-sectional view of the thigh on panel b was taken from <https://quizlet.com/gb/402555827/thigh-cross-section-diagram/>.

presented to the subjects, as shown in Fig. 5. In summary, the idea of the encoding is to represent the movement of the SRL end effector in one plane as the tactile sensation that moves around and inside-out of the cross section of the thigh. The third dimension (not tested in the present study) would be then mapped to movement along the thigh axis, in the same way as previously employed in the TR-S test.

The subjects used the SpaceMouse to control the velocity of a virtual cursor moving in the plane, simulating SRL movements. Rotating the SpaceMouse around the z-axis controlled the changes in the radial angle of the simulated SRL, while the radial distance was adjusted using the dominant method (either y-axis translation or x-axis rotation) of moving the SpaceMouse left or right. The cursor position was conveyed using the encoding described above. Notably, when adjusting the radial distance, the subjects could switch to a pad on the thigh's opposite side, facilitating quicker target reaching. Specifically, when the frequency reached the highest value on one pad and if the subject maintained the same command input, the opposite pad would be activated at the highest frequency and then the frequency would decrease moving the cursor towards the "surface" of the other side of the thigh. The cursor movement was controlled using the SpaceMouse's 'speed' setting and proportional-integral (PI) controller, which regulated cursor velocity. The velocity was integrated to determine the cursor position. Control parameters were empirically optimized during pilot tests to balance control responsiveness with feedback dynamics effectively.

During familiarization phase, the subjects learned to control the SpaceMouse at their own pace and associate the electro-tactile sensations produced by different pads and frequencies, with visual feedback on the cursor position (Fig. 5c). In the reinforced learning phase, they were asked to reach a target displayed on the screen starting from a random (but visually undisclosed) pad, while relying solely on the tactile feedback. Upon judging that the target was reached, subjects pressed the left button on the SpaceMouse, prompting a 1 s stimulation pause and visual feedback indicating the correctness of their answers. If the subject reached the correct target pad, the pad was coloured green, otherwise, the correct pad was coloured red. Subsequently, a new pseudo-randomly selected starting and target positions were designated. The total number of targets was 40 (10 pads \times 4 frequencies). The validation phase followed the same protocol (including the number of trials) but without the visual cues. The experimental session lasted between 32 and 73 min.

Data analysis

The primary outcome measure across all tests was the Success Rate (SR). In static recognition tests (SD and FD), it represented the percentage of correctly identified stimuli (active pad and frequency level, respectively). In cursor control tests (TR-S and TR-MSF), it was defined as the percentage of trials in which the subjects correctly reached the target. Marginal SR in reaching the correct pad column (SR_{pad}), regardless of the electrode row and frequency level, was calculated in TR-S and TR-MSF, respectively. Additionally, marginal SR in "reaching" the correct frequency level (SR_{freq}), regardless of the electrode pad, was calculated in TR-MSF. The percentage of overshoots, trial time and the path efficiency were also assessed in the two TR tasks. The overshoots were calculated as the percentage of successful trials where the subject initially reached the target but then continued to move throughout the grid/electrode. The trial time, i.e., the time required to reach the target, was measured from the beginning of the trial until the subject reported that the target was reached. The path efficiency was calculated as an actual path length divided by an optimal path length (minimum number of pads needed to reach the target). This measure was computed only for those trials where the subjects reached the correct target pad. The trial time and path efficiency were calculated for each admissible trial and subsequently averaged within subjects. Furthermore, in the TR-S test, an out-of-grid measure was calculated as the percentage of trials where the subjects left off the grid (i.e., the two warning pads were activated). The trial was considered successful if the participant ultimately reached the correct location, regardless of whether they got out of the grid or overshoot the target pad once or more times during the trial. Mean values and standard deviations are reported throughout the text. Finally, static information transmission (IT) was calculated for each test to assess the amount of information received, as explained in³¹. IT for each stimulus–response pair IT_{ij} was computed using the formula:

$$IT_{ij} = P_{ij} \log_2 \left(\frac{P_{ij}}{P_i} \right),$$

where P_{ij} is the joint probability of stimulus i and response j , and P_i is the a priori probability of the stimulus, calculated as the sum of the normalized probabilities for all responses to that stimulus. P_{ij} is the conditional probability of having stimulus i given the response j , calculated by dividing the joint probability by the a priori probability. In static tests, the 'stimulus' refers to the active stimulus (pad or frequency level), and the 'response' is the stimulus identified by the participant. In cursor control tests, the 'stimulus' corresponds to the target pad designated for the task, and the 'response' is the pad that the participant reached. The total IT is obtained by summing IT_{ij} values for each stimulus–response pair. Maximum IT (IT_{max}) corresponding to 100% SR, quantifying the amount of information encoded by the test, was calculated as $\log_2(n)$ where n is the number of distinct, equally likely stimuli employed in the test (shown in Fig. 3). Finally, percentage of information transmitted (pIT) was calculated as a quotient of the previous two values. The overview of all outcome measures is presented in Table 1.

Anderson–Darling test showed that data were normally distributed, and parametric tests were employed in further analysis. To assess performance disparities between closed-loop tracking with dynamic feedback and static recognition of stimuli, SR in TR-S and SD were compared using independent samples t-test. In the FD test, paired t-test was used to compare SRs from FD-SP and FD-MP. To assess the effects of adding frequency information to the spatial coding, we compared the two TR tasks while acknowledging that the two tasks employed different experimental designs. For this purpose, independent samples t-test was used to compare the marginal SR in reaching the correct pad (SR_{pad}) in TR-S and TR-MSF, as well as the average trial times and

Outcome measure	Definition	Tests
Success Rate (SR)	Percentage of correctly identified stimuli Percentage of trials in which the subjects correctly reached the target	SD, FD TR-S, TR-MFS
Marginal SR for pad (SR _{pad})	Percentage of trials reaching the correct pad column, regardless of other factors	TR-S, TR-MSF
Marginal SR for frequency (SR _{freq})	Percentage of trials reaching the correct frequency level, regardless of pad location	TR-MFS
Overshoots	Percentage of trials where the subject reached the target but continued movement	TR-S, TR-MSF
Trial Time	Time from trial start until the target was reported as reached	TR-S, TR-MSF
Path efficiency ratio	Ratio of actual path length to the minimal path length if the target pad was reached	TR-S, TR-MSF
Out-of-grid	Percentage of trials where subjects left the defined grid area	TR-S
Information Transmission (IT)	Measure of effectiveness of the communication between stimulus and response	All
Maximum IT (IT _{max})	The theoretical maximum information that can be encoded by the test, based on the number of stimuli	All
Percentage of IT (pIT)	Quotient of IT and IT _{max} , indicating the efficiency of information transmission	All

Table 1. Summary of outcome measures with corresponding definitions and applicability across different tests.

the path efficiency for the two tests. For each of these comparisons, Cohen’s d was calculated to measure the effect size of the differences.

Results

The results of the SD and TR-S tests are presented in Fig. 6. In SD test subjects were able to discriminate among 30 electrode pads with an average SR of $62.7 \pm 10.9\%$, ranging from 52.0 to 88.7%. In TR-S, they were able to correctly reach 30 electrode pads in $88.1 \pm 8.6\%$ of the trials, ranging from 74.7 to 98.7%. Figure 6c shows that the SR in recognizing 30 pads in the static condition (SD) was statistically significantly lower (t-test, $p < 0.001$) compared to the SR when reaching the same pads using closed-loop control (TR-S), with a very large effect size (Cohen’s $d = 2.59$). Confusion matrices for the two tests are presented in Fig. 6a and b. The spread around the diagonal is decreased for TR-S, indicating higher accuracy. Parallel lines adjacent to the main diagonal indicate the recognition of neighbouring pads in the same electrode row. Similarly, lines distanced by ten spaces from the main diagonal show the recognition of neighbouring pads in the same electrode column. In TR-S, subjects exhibited no overshoots in $64.1 \pm 13.7\%$ of trials and managed to stay within the grid during $50.6 \pm 30.3\%$ of trials. The average trial time was 11.0 ± 2.8 s, while the average path efficiency was 0.37 ± 0.12 .

The results of the FD test are shown in Fig. 7. The subjects could discriminate four frequency levels delivered on the same pad (FD-SP) with an average SR of $86.0 \pm 8.3\%$, ranging from 73.3 to 100.0%. Conversely, when the task involved different pads (FD-MP), the SR dropped significantly (t-test, $p < 0.01$) to $74.3 \pm 9.6\%$, ranging from 56.7 to 86.7%. The difference in SR between the two tests represents a large effect size (Cohen’s $d = 1.30$). As shown by the confusion matrices, lower frequencies were recognized more accurately in both FD-SP and FD-MP.

Figure 8 presents the results of the TR-MSF test. The figure shows the SRs for each target position in the TR task (i.e., combinations of pads and frequency levels), averaged across trials and subjects. The overall average

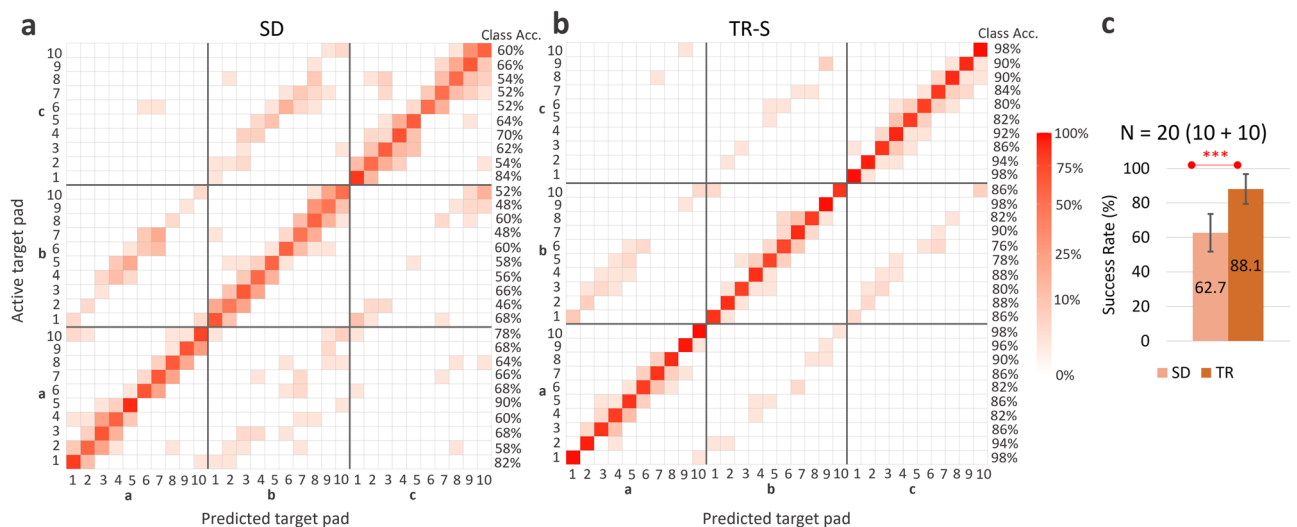


Fig. 6. The results of SD and TR-S tests: (a) Confusion matrix for the recognition of 30 pads in SD test, (b) Confusion matrix for reaching 30 target pads in TR-S test, (c) Average SRs in SD and TR-S tests showing mean and standard deviation across 10 subjects. *: Statistically significant effects are denoted by $*p < 0.05$, $**p < 0.01$, and $***p < 0.001$.

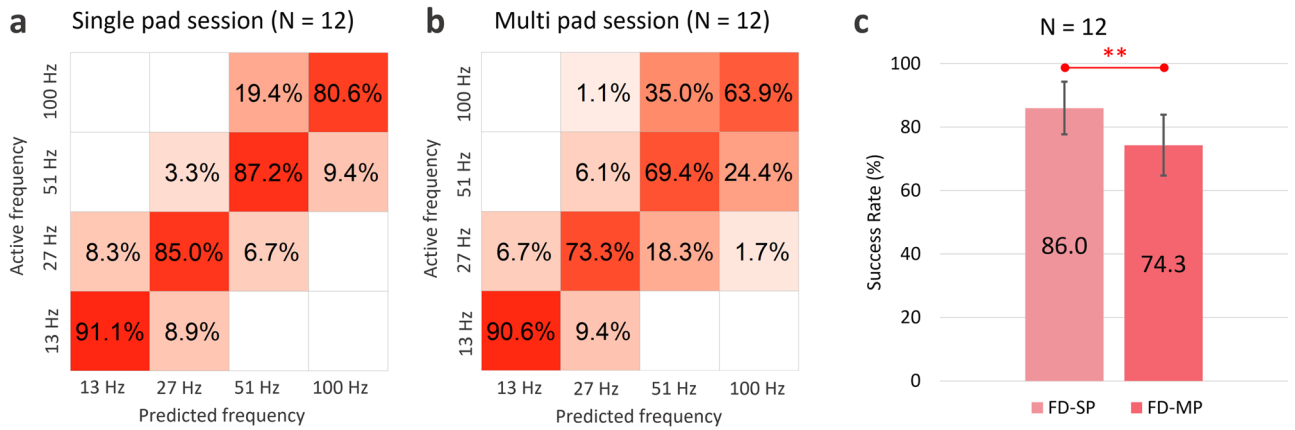


Fig. 7. The results of FD test. Confusion matrices represent Success Rate (SR) for each frequency level in (a) Single pad session and (b) Multi pad sessions of FD test (FD-SP and FD-MP, respectively). (c) The overall average SRs (mean and standard deviation) in recognizing four frequency levels across 12 subjects. *: Statistically significant effects are denoted by * $p < 0.05$, ** $p < 0.01$, and *** $p < 0.001$.

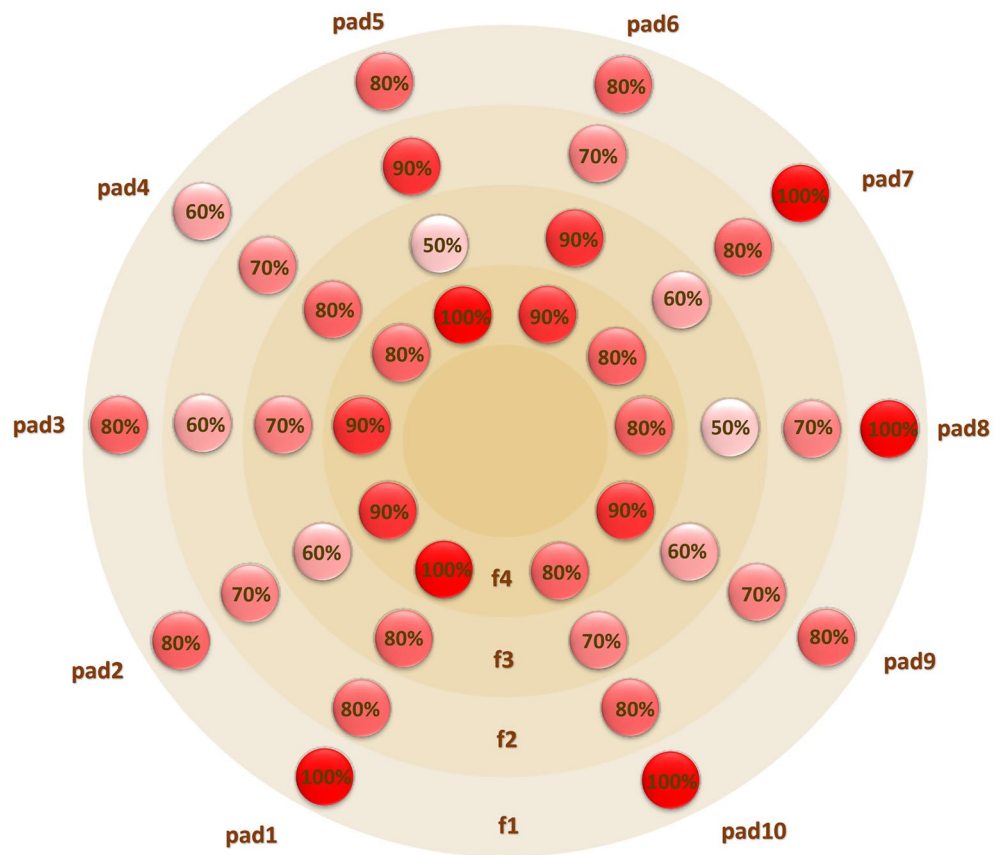


Fig. 8. The results of TR-MSF test—Success Rate (SR) for reaching each of 40 targets represented by a combination of ten electrode pads and four frequency levels.

SR to reach 40 targets was $78.8 \pm 9.8\%$, ranging from 57.5% to 92.5%. Furthermore, the overall marginal SRs for reaching the correct electrode pad regardless of frequency (SR_{pad}) was $88.2 \pm 7.6\%$, while for selecting the accurate frequency level regardless of the pad (SR_{freq}) was $88.0 \pm 5.5\%$. There were no overshoots in $48.5 \pm 11.2\%$ of trials. The average trial time to reach the target was 26.4 ± 8.5 s, and the validation phase duration was $22 \text{ min } 20 \text{ s} \pm 8 \text{ min } 11 \text{ s}$. The average path efficiency was 0.27 ± 0.09 .

The comparison of subjects' performance in reaching the correct pad (SR_{pad}), regardless of frequency in TR-MSF ($88.2 \pm 7.6\%$) and regardless of electrode row in TR-S ($91.1 \pm 7.6\%$) is presented in Fig. 9. Independent samples t-test showed no statistically significant differences between these marginal success rates, with a small to medium effect size (Cohen's $d = 0.38$). However, average trial time was significantly longer

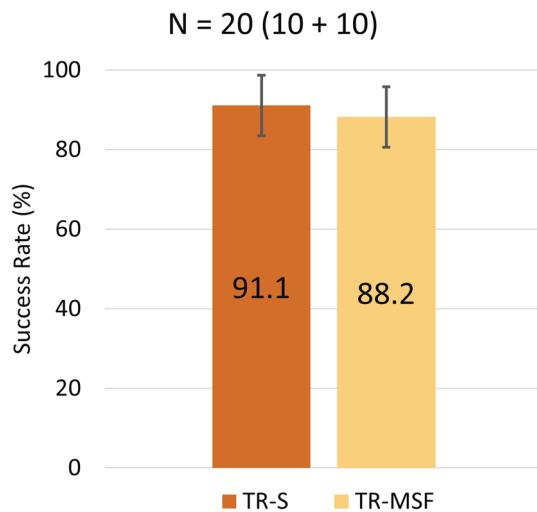


Fig. 9. The comparison of average marginal SRs in reaching the target pad location in the electrode row in TR-MSF (regardless of the frequency level) and TR-S (regardless of the electrode row). *: Statistically significant effects at $*p < 0.05$, $**p < 0.01$, $***p < 0.001$.

($p < 0.001$, Cohen's $d = 2.43$) for combined encoding: 26.4 ± 8.5 s for TR-MSF vs. 11.0 ± 2.8 s for TR-S. The t-test showed no significant differences in the path efficiencies between the two tests, although the large effect size (Cohen's $d = 0.94$) suggests a meaningful difference in practical terms.

Table 2 summarizes the results of IT calculated for all tests presented in this paper. It should be noted that in FD-MP test the subjects were presented with 120 different stimuli (30 pads \times 4 frequencies), while only reporting one of the four frequency levels, as in FD-SP.

Discussion

This paper aimed to assess the feasibility of a high-resolution electrotactile feedback interface envisioned for conveying 3D spatial information to SRL users. Four separate experiments were conducted, driven by specific hypotheses we set to investigate key aspects of the novel electrotactile interface.

Our first hypothesis was that dynamic encoding during closed loop control will feed more information to the subjects throughout the task execution, thereby improving their spatial orientation across the electrode in comparison to static recognition of stimuli. Valette et al.²⁶ evaluated spatial discrimination of multi-channel electrotactile stimulation and reported an SR of 64.55% in discriminating eight pads placed around the thigh with a 2.6 cm center-to-center distance. Our study demonstrated that similar performance ($62.7 \pm 10.9\%$) can be maintained with high-resolution interface comprising 30 pads arranged in three rows, with a center-to-center distance of 4.1 cm in each row. The results from the TR-S highlighted a significant improvement in subjects' ability to reach the specific target pad among 30 electrode pads ($88.1 \pm 8.6\%$) compared to the identification of a specific static stimuli location in the SD test for the same number and arrangement of pads. The amount of information received by the subjects was also similar in the two tasks (4.20 bit vs 3.26 bit). Dynamic conditions seemingly enabled subjects to perceive transitions between pads more effectively, facilitating an integrated understanding of movement and control inputs, which likely contributed to the improved performance. A study by Malesevic et al.³², compared recognition of six spatial locations using static encoding with six dynamic patterns on the torso, revealing significantly better results with the dynamic approach, even without relying on the closed-loop control. Similarly, Hu et al.³³ showed the dynamic approach drastically improves understanding of electrotactile patterns on wrist, compared to the static approach. This is an encouraging result for the online application of the designed electrotactile interface confirming that high identification of randomly activated pads is not a requirement for good online control.

The performance in frequency discrimination in FD-SP are slightly lower than those reported by Strbac et al.⁸ where four frequency levels were recognized with $95 \pm 8\%$ success rates on the forearm. Although direct

Test	SD (n = 30)	TR-S (n = 30)	FD-SP (n = 4)	FD-MP (n = 4)	TR-MSF (n = 40)
IT (bit)	3.26	4.20	1.36	1.07	4.47
Max IT (bit)	4.91	4.91	2.00	2.00	5.32
pIT (%)	66.39	85.54	68.00	53.50	84.02

Table 2. Static information transmission (IT), maximum IT and percentage of information transmitted (pIT) for all conducted tests with n different stimuli.

comparisons between different electrode positions and topologies is difficult, these results are not surprising considering higher frequency levels used in present study. Our second hypothesis was that the recognition of frequency would be more challenging when this task is performed over complete electrode matrix. Indeed, the FD test demonstrated that changing the pads during frequency recognition negatively affected the performance (FD-MP vs. FD-SP), measured by both SR and IT. This is likely due to the variations in sensory perception across distinct thigh regions²² but could be also affected by the training process as the two sessions were matched in the number of trials, hence resulting in more focused training in FD-SP. Analysis of the SRs across four frequency levels in both FD-SP and FD-MP indicates that the JND function, derived from the study performed on the forearm, may not be ideally suited for the thigh electrode used in our study. Notably, the differences in SR among frequency levels were less pronounced in the FD-SP. However, we observed a significant decrease in frequency recognition from lower to higher frequencies in the FD-MP test, suggesting that perceptual variations across pads impair discrimination, particularly at the higher frequencies. This result is important for the real-world applicability of the system which will inevitably include activation of multiple pads. Nevertheless, the perceived drop in performance is relatively modest (13.6%) and it should be also considered that online application allows the subject to use transitions and their own commands to improve the recognition, which can compensate for relatively minor drop in performance. Indeed, when the closed-loop control was enabled (TR-MFS), the SR in recognizing frequency levels across different pad locations increased. Namely, marginal SR for identifying four frequency levels in the TR-MSF test reached $88.0 \pm 5.5\%$, surpassing even the outcomes of FD-SP (recognition in static condition). This aligns with the previous comparisons between the TR-S and SD tests and demonstrates the superiority of dynamic encoding which allows the user to feel transitions and better locate the target pad/frequency. Overall, this gives a positive outlook towards the applicability of the system even with a reduced calibration and training time (i.e., training on a single pad prior to using all pads).

Lastly, considering that the stimuli location and frequency can be perceived as independent parameters, the goal was to combine them to convey the feedback on 3D position in a cylindrical coordinate system. We have tested the discrimination of position and frequency within the simplified 2D closed loop task as the extension to the third dimension is assumed to be simple (activating across rows). Our third hypothesis was that including frequency information in the combined dynamic encoding will not compromise the accuracy observed when using only the spatial modality. Although TR-S and TR-MSF test cannot be compared directly due to different design and protocol, obtained results speak in favour of this hypothesis. Both tests were essentially based on TR task between the same 10 points, with two additional electrode rows (TR-S) or three additional frequency levels (TR-MSF). The results showed similar performance despite a larger variety of stimuli in TR-MSF. This implies that mixed encoding facilitates the closed-loop control task. It should be noted that the total number of targets, and therefore the potential “distance” between the start and target position is increased in the TR-MSF compared to TR-S test (40 vs. 30-point matrix). Consequently, TR-MSF further allowed subjects to receive more information compared to TR-S, but also resulted in lower path efficiency. Another important difference between the two tasks is the control interface (SpaceMouse in TR-MSF and the keyboard in TR-S). The mouse controlled the velocity of the cursor and the subjects had to rely on the electro tactile stimulation to estimate the position. In contrast, during keyboard control, the subject controlled the position directly, i.e., a single arrow press corresponded to a single pad movement. This allowed the subjects to gauge their movements by counting keystrokes, without entirely relying on tactile feedback throughout the movement. The difference in the control interface is also why the trial time was longer in the TR-MSF test compared to the TR-S test (the cursor movement was generally slower). It's important to note that precise control is not a strict requirement for the application of interest as well as that the control system was not optimized for rapid movements. This is not a limitation given that robotic arm movements are generally slower than those of humans (e.g., 300 mm/s for the robot arm and 650–1300 mm/s in humans³⁴).

We assume that relatively high SR in TR-MSF test is in part the result of the electrode design and feedback coding. For example, the employed coding using the polar coordinates allowed subjects to move to the opposite pad in the TR-MSF test, switching from the highest frequency on a pad from one side of the thigh to the highest frequency on the pad which is on the opposite side of the thigh. This corresponds to the radial movement along the same direction in the polar coordinate system. Therefore, the same control input will result in different feedback, i.e., change of pad instead of the frequency increase, and in this way, the employed feedback design provides additional cues which potentially facilitated the navigation. Specifically, for subjects it was easy to recognize that when the pad changed to the opposite side of the thigh, the frequency was at the highest level. We hypothesized that this in part contributed to the better outcomes compared to the FD test. Furthermore, due to variations in the circumference of each leg, some participants had a larger gap between the first and last pad, i.e. leg circumference was not fully covered by electrodes, resulting in a more distinct sensation between these two pads compared to any other pair. Impression of multiple subjects was that these two pads served as points of orientation in some of the trials, which is supported by the fact that pad 1 and pad 10 exhibited the highest SR in the TR-MSF test.

We should emphasize that our decision to utilize only 10 electrode pads in the TR-MSF test, compared to the full array of 30 pads, reflects the balance between task duration and subject engagement. However, incorporation of the third spatial dimension is unlikely to have a substantial impact due to the presumed independence of spatial and frequency channels in electro tactile stimulation. Considering the unique tactile sensations elicited by varying frequency levels, it is theoretically plausible to propose that the SR for a holistic 3D testing framework, integrating both spatial dimensions and frequency variations, could be estimated by multiplying the SRs obtained from the separate TR-S and TR-MSF tests. This proposal assumes that the processes underlying spatial and frequency recognition operate independently and do not influence each other's outcomes. However, it's important to note that this hypothesis, while grounded in the observed independence of tactile sensations in our preliminary tests, requires empirical validation through comprehensive 3D testing.

Future research will explore the application of the 3D feedback interface in real-time closed-loop control scenario with SRL or another type of a robotic manipulator⁹. Previously, vibrotactile feedback was successfully used for conveying the 2D position of a robotic arm, sharing the workspace with the user upper limbs, during an online tracking task²³, as well as for the interaction force of the wearable SRL during force-regulation task³⁵. However, these haptic interfaces used only four channels for transmitting position and one for force. Our assumption is that the high-resolution system can provide significant benefits during the control of 3D movement and grasping force of a wearable SRL. It is also important to assess how such feedback impacts embodiment and motor control especially when used longitudinally¹⁹ in the relevant environment. Therefore, future efforts will aim not only to advance SRL technologies but also to provide valuable insights into the broader implications of enhanced feedback mechanisms in human–machine interfaces.

Data availability

Data sets generated during the current study are available from the corresponding author on reasonable request.

Received: 15 April 2024; Accepted: 22 August 2024

Published online: 28 August 2024

References

- Szeto, A. Y. J. & Saunders, F. A. Electrocutaneous stimulation for sensory communication in rehabilitation engineering. *IEEE Trans. Biomed. Eng.* **BME-29**, 300–308 (1982).
- Trout, M. A., Harrison, A. T., Brinton, M. R. & George, J. A. A portable, programmable, multichannel stimulator with high compliance voltage for noninvasive neural stimulation of motor and sensory nerves in humans. *Sci Rep* **13**, 3469 (2023).
- D'Alonzo, M., Dosen, S., Cipriani, C. & Farina, D. HyVE: Hybrid vibro-electrotactile stimulation for sensory feedback and substitution in rehabilitation. *IEEE Trans. Neural Syst. Rehabil. Eng.* **22**, 290–301 (2014).
- Chouvardas, V. G., Miliou, A. N. & Hatalis, M. K. Tactile displays: Overview and recent advances. *Displays* **29**, 185–194 (2008).
- Li, K., Boyd, P., Zhou, Y., Ju, Z. & Liu, H. Electrotactile feedback in a virtual hand rehabilitation platform: Evaluation and implementation. *IEEE Trans. Autom. Sci. Eng.* **16**, 1556–1565 (2019).
- Abbass, Y., Seminara, L., Saleh, M. & Valle, M. Novel wearable tactile feedback system for post-stroke rehabilitation. In *2021 IEEE Biomedical Circuits and Systems Conference (BioCAS)* 1–6 (IEEE, 2021). <https://doi.org/10.1109/BioCAS49922.2021.9645020>.
- Dosen, S. *et al.* Multichannel electrotactile feedback with spatial and mixed coding for closed-loop control of grasping force in hand prostheses. *IEEE Trans. Neural Syst. Rehabil. Eng.* **25**, 183–195 (2017).
- Štrbac, M. *et al.* Integrated and flexible multichannel interface for electrotactile stimulation. *J. Neural Eng.* **13**, 046014 (2016).
- Štrbac, M. *et al.* Short- and long-term learning of feedforward control of a myoelectric prosthesis with sensory feedback by amputees. *IEEE Trans. Neural Syst. Rehabil. Eng.* **25**, 2133–2145 (2017).
- Garenfeld, M. A., Mortensen, C. K., Štrbac, M., Dideriksen, J. L. & Dosen, S. Amplitude versus spatially modulated electrotactile feedback for myoelectric control of two degrees of freedom. *J. Neural Eng.* **17**, 046034 (2020).
- Patel, G. K., Dosen, S., Castellini, C. & Farina, D. Multichannel electrotactile feedback for simultaneous and proportional myoelectric control. *J. Neural Eng.* **13**, 056015 (2016).
- Pamungkas, D. & Ward, K. Electro-tactile feedback for tele-operation of a mobile robot. In *Australasian Conference on Robotics and Automation* 1–7 (University of New South Wales, 2013).
- Cheng, S. & Zhang, D. A wearable armband “iFeel” for electrotactile stimulation. In *2017 10th International Conference on Human System Interactions (HSI)* 120–124 (IEEE, 2017). <https://doi.org/10.1109/HSI.2017.8005012>.
- Pamungkas, D. & Ward, K. Immersive teleoperation of a robot arm using electro-tactile feedback. In *2015 6th International Conference on Automation, Robotics and Applications (ICARA)* 300–305 (IEEE, 2015). <https://doi.org/10.1109/ICARA.2015.7081164>.
- Pamungkas, D. S. & Ward, K. Electro-tactile feedback system to enhance virtual reality experience. *IJCTE* **8**, 465–470 (2016).
- Vizcay, S., Kourtesis, P., Argelaguet, F., Pacchierotti, C. & Marchal, M. Electrotactile feedback for enhancing contact information in virtual reality. In *ICAT-EGVE 2021—International Conference on Artificial Reality and Telexistence and Eurographics Symposium on Virtual Environments*. <https://doi.org/10.2312/EGVE.2021.1331> (2021).
- NIMA—An EU H2020 Research and Innovation Action. <https://nima-project.eu/index.php/contact/>.
- Prattichizzo, D. *et al.* Human augmentation by wearable supernumerary robotic limbs: Review and perspectives. *Prog. Biomed. Eng.* **3**, 042005 (2021).
- Pinardi, M. *et al.* Impact of supplementary sensory feedback on the control and embodiment in human movement augmentation. *Commun. Eng.* **2**, 64 (2023).
- Sobajima, M., Sato, Y., Xufeng, W. & Hasegawa, Y. Improvement of operability of extra robotic thumb using tactile feedback by electrical stimulation. In *2015 International Symposium on Micro-NanoMechatronics and Human Science (MHS)* 1–3 (IEEE, 2015). <https://doi.org/10.1109/MHS.2015.7438269>.
- Segura Meraz, N., Sobajima, M., Aoyama, T. & Hasegawa, Y. Modification of body schema by use of extra robotic thumb. *Robomech. J.* **5**, 3 (2018).
- Boljanić, T. *et al.* Design of multi-pad electrotactile system envisioned as a feedback channel for supernumerary robotic limbs. *Artif. Organs* **46**, 2034–2043 (2022).
- Pinardi, M., Noccaro, A., Raiano, L., Formica, D. & Di Pino, G. Comparing end-effector position and joint angle feedback for online robotic limb tracking. *PLoS ONE* **18**, e0286566 (2023).
- Wang, W. *et al.* Building multi-modal sensory feedback pathways for SRL with the aim of sensory enhancement via BCI. In *2019 IEEE International Conference on Robotics and Biomimetics (ROBIO)* 2439–2444 (IEEE, 2019). <https://doi.org/10.1109/ROBIO49542.2019.8961383>.
- Solomonow, M., Lyman, J. & Freedy, A. Electrotactile two-point discrimination as a function of frequency, body site, laterality, and stimulation codes. *Ann. Biomed. Eng.* **5**, 47–60 (1977).
- Valette, R., Gonzalez-Vargas, J. & Dosen, S. The impact of walking on the perception of multichannel electrotactile stimulation in individuals with lower-limb amputation and able-bodied participants. *J. NeuroEng. Rehabil.* **20**, 108 (2023).
- Webb, G. D., Ewins, D. J. & Ghousayni, S. Electro-tactile sensation thresholds for an amputee gait-retraining system (2012).
- Company website. <https://policrom.it/en/homepage/>.
- TACTILITY—An EU H2020 Research and Innovation Action. <https://tactility-h2020.eu/>.
- Isakovic, M., Malesevic, J., Kostic, M., Dosen, S. & Štrbac, M. The impact of size and position of reference electrode on the localization of biphasic electrotactile stimulation on the fingertips. *IEEE Trans. Haptics* **15**, 255–266 (2022).
- Barralon, P., Ng, G., Dumont, G. A., Schwarz, S. K. W. & Ansermino, J. M. Design of rhythm-based vibrotactile stimuli around the waist: Evaluation of two encoding parameters. *IEEE Trans. Syst. Man Cybern. A* **39**, 1062–1073 (2009).

32. Malešević, J. *et al.* Electrotactile communication via matrix electrode placed on the torso using fast calibration, and static vs. *Dyn. Encoding Sens.* **22**, 7658 (2022).
33. Hu, X., Lu, X. & Sun, H. The wearable tactile information expression system based on electrotactile rendering. In *Transactions on Edutainment XIII* (eds. Pan, Z., Cheok, A. D., Müller, W. & Zhang, M.) Vol. 10092 46–53 (Springer, 2017).
34. Matic, A., Valerjev, P. & Gomez-Marin, A. Hierarchical control of visually-guided movements in a 3D-printed robot arm. *Front. Neurobot.* **15**, 755723 (2021).
35. Buratti, S. *et al.* Effect of vibrotactile feedback on the control of the interaction force of a supernumerary robotic arm. *Machines* **11**, 1085 (2023).

Acknowledgements

This work was supported by the European Commission under the “NIMA: Non-invasive Interface for Movement Augmentation” project (H2020-FETOPEN-2018-2020, ID: 899626). We thank our colleague Filip Budimir for the help in creation of Figure 1 and all the participants who devoted their time to take part in the experiments presented in this manuscript.

Author contributions

M.K. and M.S. conceptualized and designed the system, P.B. adapted the stimulator, T.B., M.B. and M.S. designed the electrodes, T.B., M.S. and S.D. conceived the experiments, T.B. M.B. and M.K. conducted the experiments, T.B., M.B. and P.B. analysed the results, T.B., M.B. and M.S. prepared the publication. All authors reviewed the manuscript.

Competing interests

The authors declare no competing interests.

Additional information

Correspondence and requests for materials should be addressed to T.B.

Reprints and permissions information is available at www.nature.com/reprints.

Publisher's note Springer Nature remains neutral with regard to jurisdictional claims in published maps and institutional affiliations.

Open Access This article is licensed under a Creative Commons Attribution-NonCommercial-NoDerivatives 4.0 International License, which permits any non-commercial use, sharing, distribution and reproduction in any medium or format, as long as you give appropriate credit to the original author(s) and the source, provide a link to the Creative Commons licence, and indicate if you modified the licensed material. You do not have permission under this licence to share adapted material derived from this article or parts of it. The images or other third party material in this article are included in the article's Creative Commons licence, unless indicated otherwise in a credit line to the material. If material is not included in the article's Creative Commons licence and your intended use is not permitted by statutory regulation or exceeds the permitted use, you will need to obtain permission directly from the copyright holder. To view a copy of this licence, visit <http://creativecommons.org/licenses/by-nc-nd/4.0/>.

© The Author(s) 2024